

Rationale

Lyman-break galaxies (LBG) represent by far the most numerous population of galaxies that we are able to observe in the early Universe. Estimates of dust extinction are needed to convert the UV luminosity density into a star-formation rate density (SFRD), and to constrain the amount of obscured star formation occurring in different systems at high redshift. To investigate the dust content of LBGs, great attention has been devoted to the study of the slope of the UV continuum (β) which is mainly determined by dust absorption, but is also affected by other physical parameters, above all metallicity and age. For a given extinction both lower metallicity stars and young ages are responsible for bluer UV slopes, while the contribution from nebular continuum produces a reddening of β . As recently noted by Wilkins et al. (2013) on the basis of galaxy formation models, any variation with redshift of the above factors can introduce systematic biases in the computation of dust extinction and of the corrected SFRD. Unfortunately, photometric data alone do not allow us to determine how different properties shape the observed UV slope. In particular, while deep IR photometry leads to tighter constraints on the age of the stellar populations, stellar metallicity remains very poorly constrained even in the deepest photometric datasets.

We analyse here a unique sample of galaxies at $z > 2.9$ for which not only redshift but also metallicity (either stellar or gas-phase) has been measured, and exquisite deep photometry is available in all bands, from the optical to the crucial IR. The availability of CANDELS WFC3 observations, of the deep K-band data of the HUGS-CANDELS survey (Fontana et al. 2014), and of IRAC/SEDs data allows us to accurately sample the Balmer break at these redshifts to constrain the age of the objects in our sample. The available multi-wavelength data covering the rest-frame UV are exploited to estimate extinction from the slope of the continuum under commonly adopted assumptions in order to compare the SFR derived by correcting the UV luminosity to the SFR obtained through an SED-fitting performed while fixing the metallicity of population synthesis models to the measured one.

Objects at $z \sim 3-4$ with metallicity from deep spectroscopy

We consider objects at $z \sim 2.9-3.8$ in the GOODS-S field for which a spectroscopic estimate of their stellar and/or gas phase metallicity is available. The sample includes seven objects with measured stellar metallicity from UV absorption features: the subsample of four LBGs at $3.4 < z < 3.8$ in the CDFS from the AMAZE survey (Maiolino et al. 2008) presented in Sommariva et al. (2012) (hereafter S12), and three galaxies at $2.9 < z < 3.4$ from the public release of the GMASS survey (Kurk et al. 2013) whose stellar metallicity estimates are presented here for the first time.

Stellar metallicities are measured from the equivalent width of photospheric absorption lines sensitive to metallicity and independent to the other stellar parameters such as age and initial mass function (IMF). Gas-phase metallicity has been measured from diagnostics based on the [OII]3727, [OIII]5007, and H β emission lines.

The objects that we have selected are reasonably representative of the general population of bright LBGs. All 14 galaxies have subsolar metallicity in the range $Z=0.07-0.39 Z_{\odot}$.

Photometric data available for the objects include CANDELS WFC3/IR observations of the GOODS-S field in the F105W, F125W and F160W bands (Koekemoer et al. 2011, Grogin et al. 2011), HST/ACS GOODS observations in the F435W, F606W, F775W, and F850LP bands; Ks-band data acquired as part of the HAWK-I UDS and GOODS-S survey (HUGS, Fontana et al. 2014) reaching $\text{mag}=26.5$ AB at $S/N=5$; Spitzer/IRAC 3.6 μm and 4.5 μm observations from the Spitzer Extended Deep Survey (SEDS, Ashby et al. 2013), reaching 5σ depths of 26.25 and 26.52 AB magnitudes in 1 FWHM aperture.

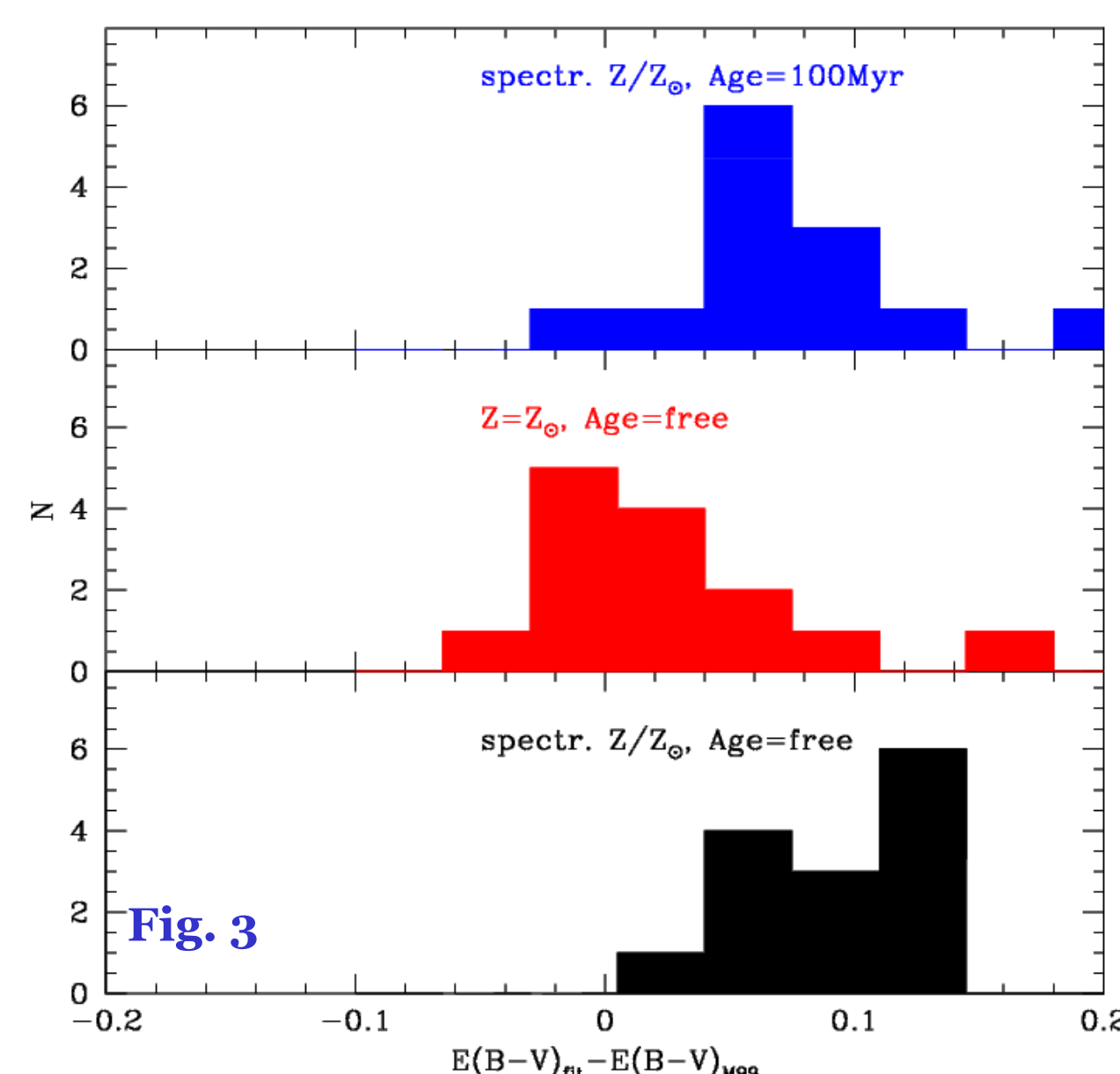
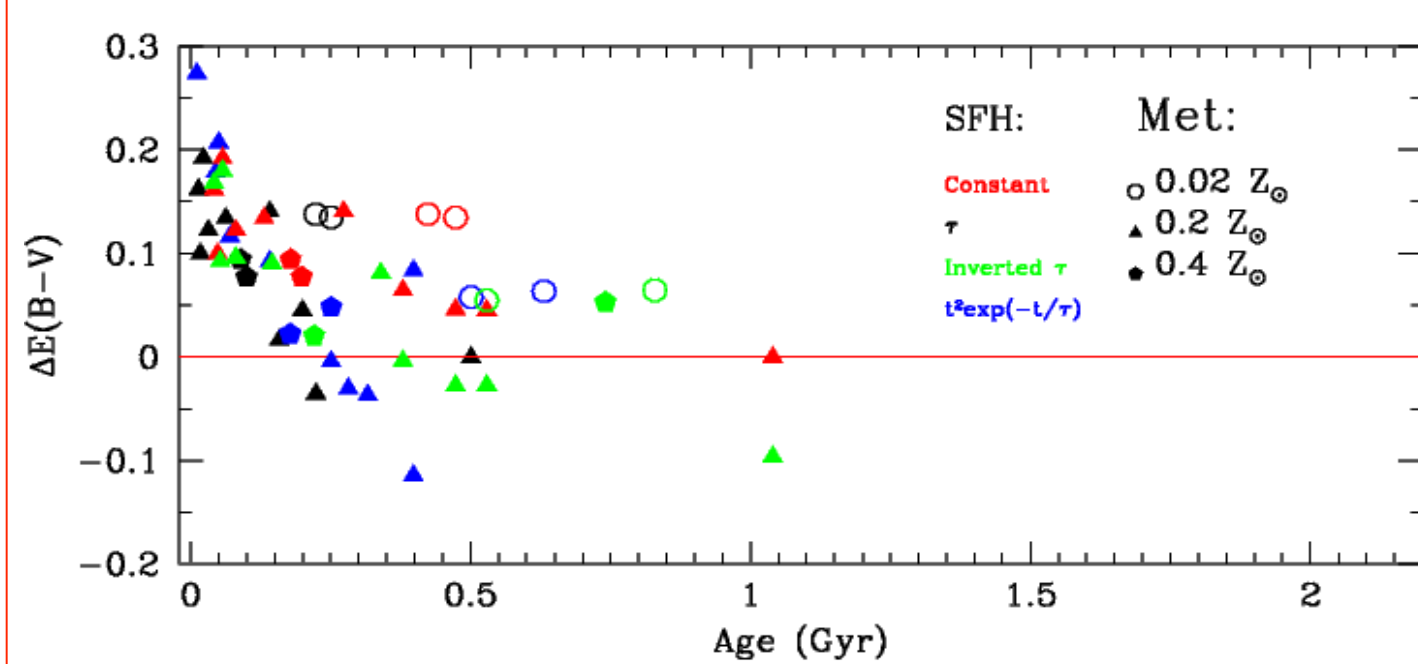
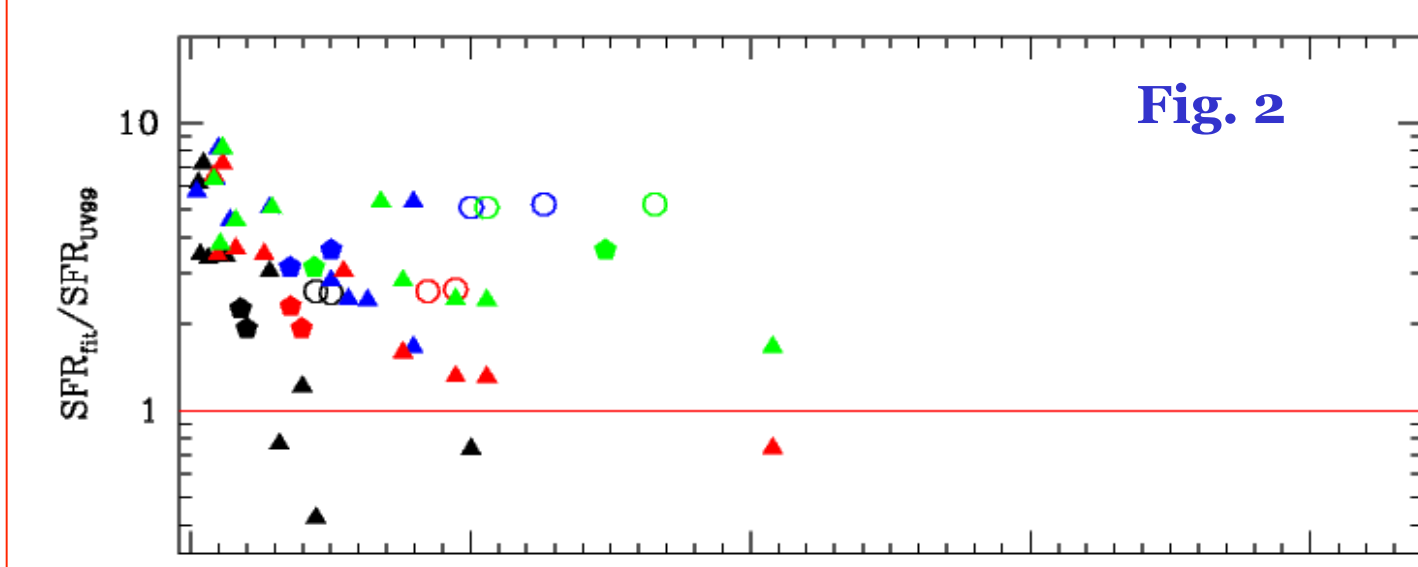
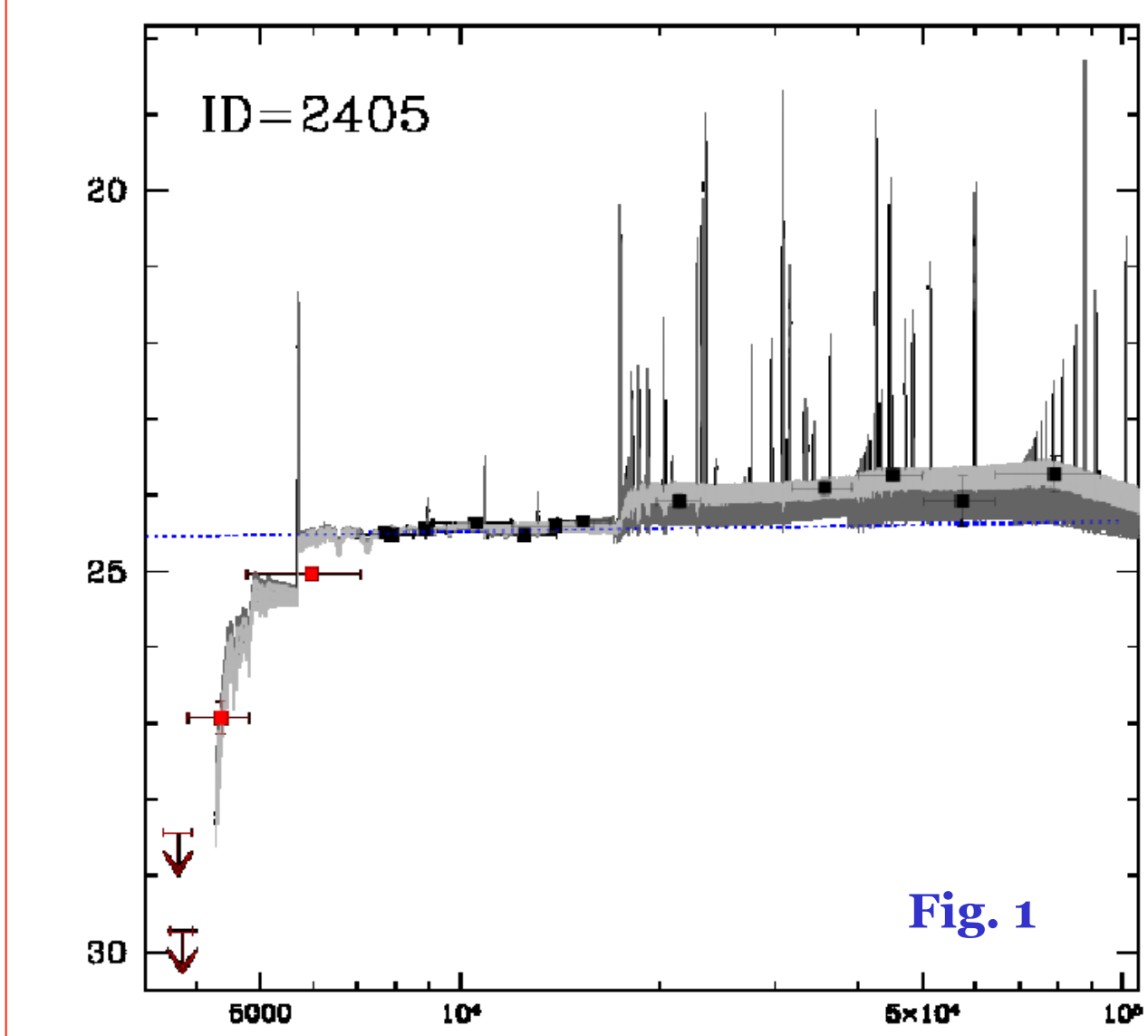
Physical properties

We estimate physical parameters by fitting the observed photometry with the Bruzual & Charlot (2003) synthetic models. In the fitting procedure for each object we fixed the redshift to the spectroscopic value and the stellar metallicity to the value nearest to the measured metallicity among the ones available in the BC03 library. We adopt four different parametrisations for the star-formation history (SFH): constant; exponentially declining; exponentially rising; and delayed SFH. We also include the contribution from nebular continuum and line emission computed following Schaerer & de Barros (2009). Nebular emission is directly linked to the amount of hydrogen-ionizing photons in the stellar SED. We adopt the common power-law approximation for the UV spectral range $F_{\lambda} \sim \lambda^{-\beta}$ and estimate the slope β of our objects by fitting a linear relation through the observed magnitudes spanning the UV rest-frame wavelength range of the objects.

As an example we show in Fig. 1 the spectral-energy distributions of object ID=1405: light (dark) grey curves in each plot show models with $P(\chi^2) > 32\%$ from the best fit, considering all four different SFH and fits with stellar (stellar+nebular) emission. The best-fit UV slope is shown as a blue dashed line.

We exploit the measured values of the UV slope to estimate extinction and colour excess following Meurer et al. 1999 ($E(B-V)_{M99}$), and we estimate the star-formation rate of the objects following Madau 1998 after correcting the UV emission on the basis of $E(B-V)_{M99}$ we refer to the star-formation rate estimated from the observed UV applying M99+Ma98 conversion equations as SFR_{UV99} .

In Fig. 2 we show the comparison between SED-fitting (without nebular emission) and UV-based extinction and SFR estimates for the 14 objects in the sample: $\Delta E(B-V) = E(B-V)_{\text{fit}} - E(B-V)_{M99}$ (bottom panel) and $\text{SFR}_{\text{fit}}/\text{SFR}_{UV99}$ (top panel). We show for each of the 14 objects the results obtained for each of the four different SFH (indicated by different colours: see inset) as a function of the relevant best-fit Age. SED fitting has been computed while fixing metallicity of models to the values closest to the measured ones (as indicated by the different symbols in the inset). The same comparison based on stellar+nebular SED-fitting yields similar results. Regardless of the assumed SFH, the $E(B-V)_{M99}$ appear to be underestimated by $\Delta E(B-V) \sim 0.05 - 0.2$, with the discrepancy being slightly larger for stellar SED models with the lowest best-fit age. We find a systematic offset between the extinction corrected SFR_{UV99} and SFR_{fit} with SED fitting indicating SFRs higher by a factor of 2-3 (nebular+ stellar SEDs) up to 8-10 (stellar SEDs) at age 10-50 Myr.



What is the origin of these discrepancies?

The conversion factors presented in Madau 1998 assume solar metallicity populations with constant SFH. The Meurer 1999 relation, which has been calibrated on local galaxies, implies a UV slope for naked stellar populations $\beta_{\text{dust-free}} = -2.23$. This value is consistent with the expected dust-free slope of a solar metallicity, age > 100 Myr population (see also Bouwens et al. 2009), raising doubts on the applicability of this relation for high- z galaxies (Wilkins et al. 2013).

The straightforward explanation for the discrepancies found between $E(B-V)_{\text{fit}}$ and $E(B-V)_{M99}$, and between SFR_{fit} and SFR_{UV99} thus lies in the difference between the subsolar metallicity of the objects in our sample and the solar metallicity used or implied by conversion equations.

We perform a simple test to constrain this scenario, in particular to assess whether allowing for young formation ages in the fit also plays a significant role in determining this result. We determine the best-fit model for each object by 1) fixing age=100 Myr with constant SFH (as assumed in deriving UV-based conversion factors), and 2) fixing metallicity to the solar value while leaving age as a free parameter.

The result of this test is shown in Fig. 3: the best-fit age=100 Myr, constant SFH models have $E(B-V)_{\text{fit}}$ significantly different from the $E(B-V)_{M99}$ obtained through M99 fitting formula (top panel), as is the case for the best-fit models (bottom panel). The best-fit solar metallicity models yield $E(B-V)_{\text{fit}}$ in much better agreement with $E(B-V)_{M99}$ (central panel).

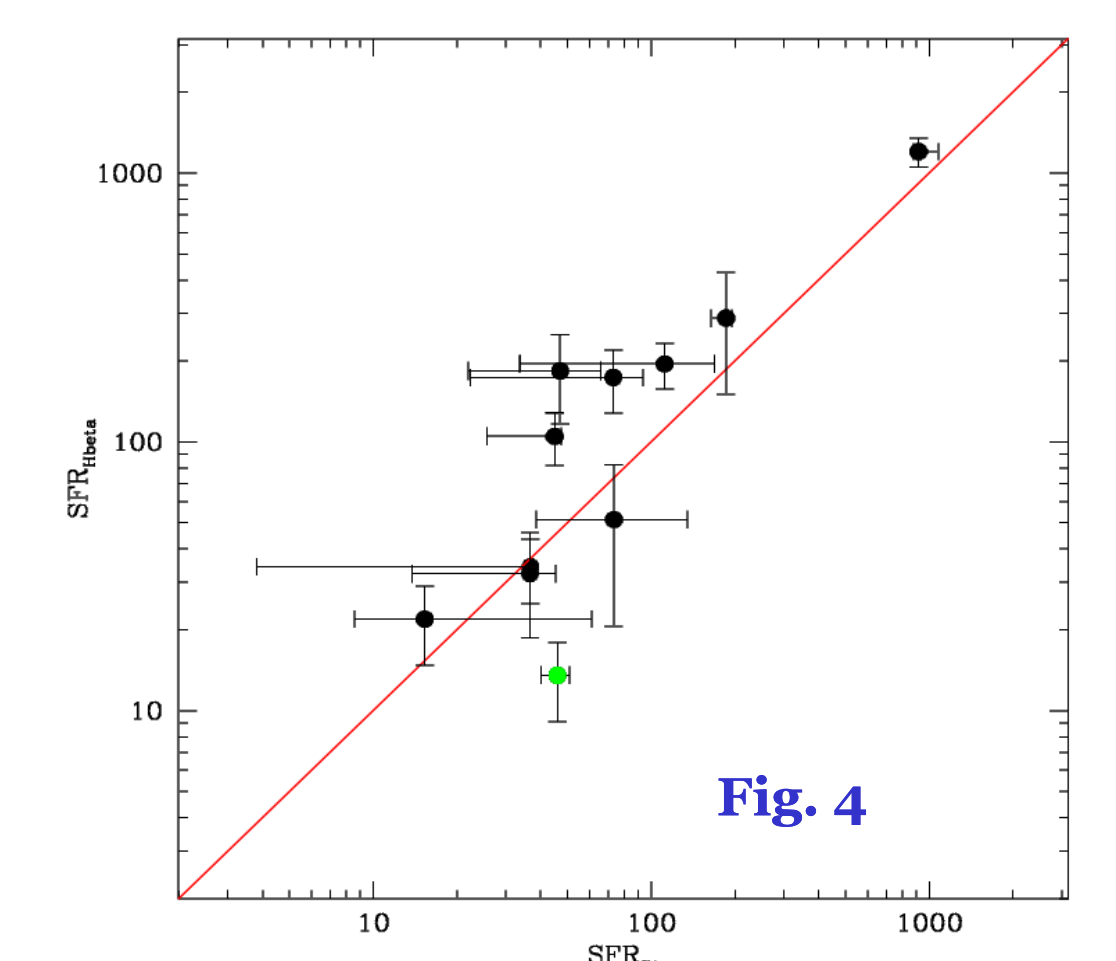
On the basis of this test we can conclude that the standard relation between UV slope and extinction (M99, implying solar metallicity SEDs) yields significant underestimates of dust corrected star-formation rates, at least for the objects considered here.

Independent constraints on the star formation rate

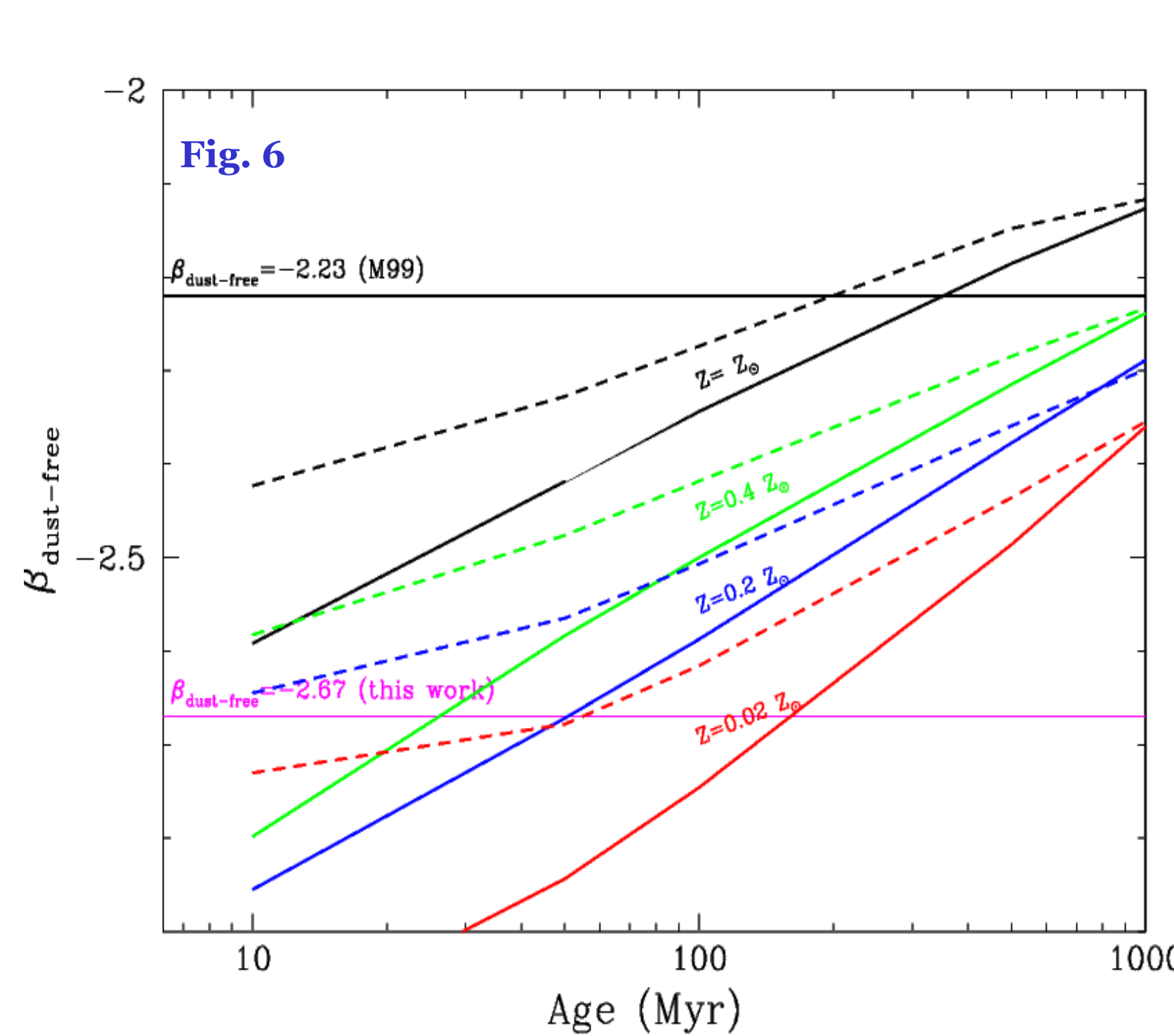
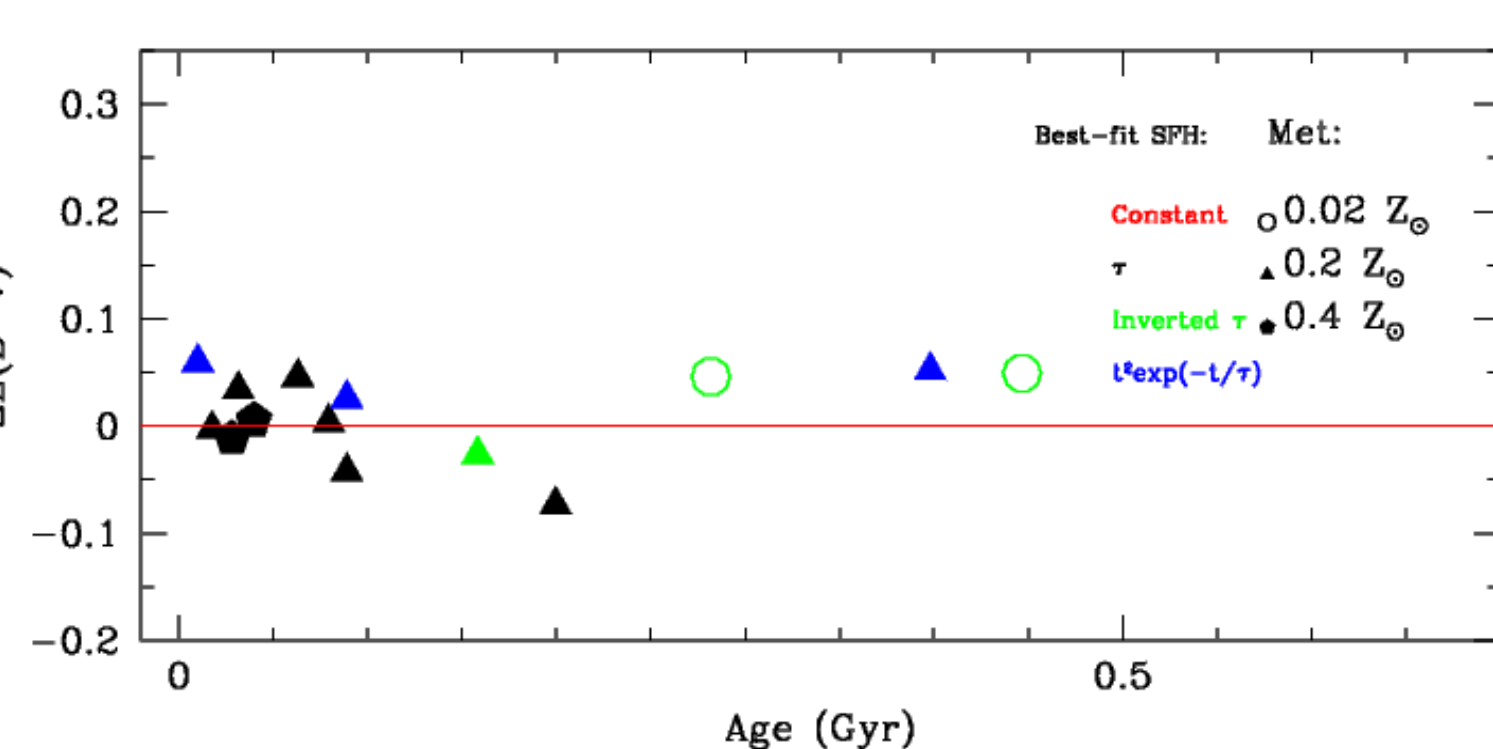
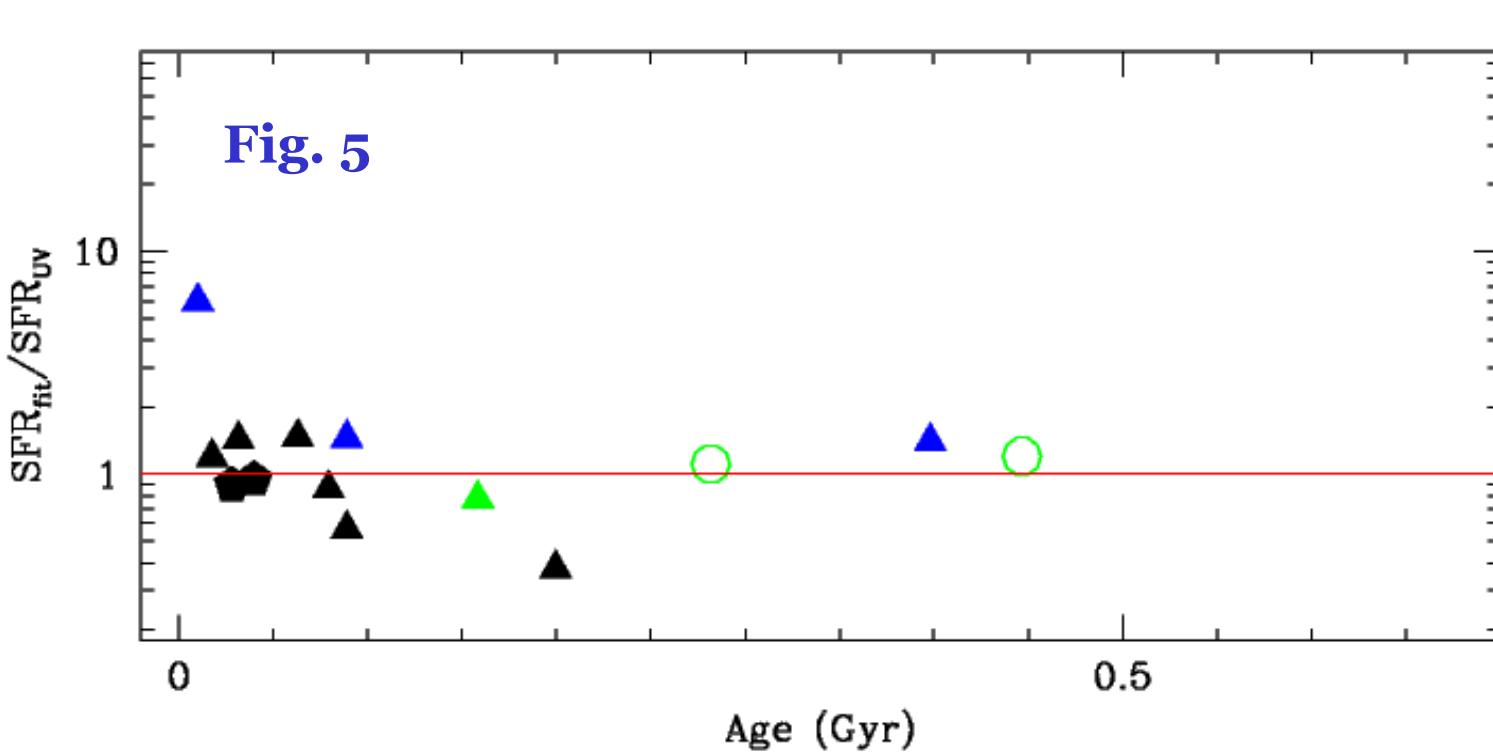
The availability of deep observations from the radio and far-IR to the X-ray allows us to put independent constraints on the SFR. Object CDFS-4417 is detected in X-ray, radio (VLA) and Herschel PACS (at 100 μm and 160 μm). On the basis of the X-ray colours and of the low X-ray to z- and H-band flux ratios, Fiore et al. 2012 conclude that the X-ray emission of CDFS-4417 is due to stellar sources rather than to a nuclear source. We estimate $\text{SFR}_{X \sim 630 \text{ GHz}} \sim 630 \pm 200 \text{ Msun/yr}$; $\text{SFR}(1.4\text{GHz}) \sim 600 \text{ Msun/yr}$, and from Herschel fluxes $\text{SFR} \sim 600-1000 \text{ Msun/yr}$ (depending on the adopted FIR templates). The SED-fitting based $\text{SFR}_{\text{fit}} \sim 900 \text{ Msun/yr}$ agrees with these independent estimates, while the SFR_{UV99} is $> 2-3$ times lower.

The other objects in our sample are not detected in the PACS images. We exploit the public PACS data to build a stacked far-IR image of the 13 objects that are not individually detected: we find a 2σ detection in both the 100 μm and 160 μm stackings. These fluxes imply a $\text{SFR} \sim 70-170 \text{ Msun/yr}$, considering the stacked object to be at the median redshift of the sample: despite the large uncertainty, this estimate is consistent with the SFR range indicated by the SED-fitting, while being 3-5 times higher than the SFR_{UV99} estimate.

We finally computed star-formation rates for the 11 objects in the AMAZE sample from the relevant H β fluxes measured in 1 arcsec apertures. As shown in Fig. 4 we find a good agreement between SFR_{fit} and $\text{SFR}_{H\beta}$. Most importantly this test confirms that the objects in our sample are dominated by young stellar populations, being recombination lines tracers of the star-formation rate on a $t < 20 \text{ Myr}$ timescale.



A revised $A_{1600} - \beta$ relation



Motivated by the results discussed above we determine a more appropriate conversion between UV slope and $E(B-V)$ on the basis of the average $\Delta E(B-V) = E(B-V)_{\text{fit}} - E(B-V)_{M99} = 0.092$ for the objects in our sample.

This $\Delta E(B-V)$ translates into an extra $\Delta A_{1600} = 0.89$ which leads to the modified $A_{1600} - \beta$ relation:

$$A_{1600} = 5.32 + 1.99\beta$$

This relation implies that the UV slope of dust-free objects is $\beta_{\text{dust-free}} = -2.67$, significantly bluer than the "zero-point" $\beta_{\text{dust-free}} = -2.23$ originally included in the M99 formula.

We also assessed whether the L_{UV} -SFR conversion factor from Madau 1998 is appropriate for our sample. By exploiting the relevant best-fit BC03 templates we computed the median L_{UV} -SFR conversion for our objects, which turns out to be 5% higher than the Madau 1998 one.

As shown in Fig. 5, when SFR_{UV} is computed on the basis of our new relation, and applying the above mentioned median L_{UV} -SFR conversion, systematic discrepancies with respect to SFR_{fit} are eliminated (the best fit model are shown for each of the 14 sources).

A check on models from the BC03 library shows that both the and the median L_{UV} -SFR conversion we find are consistent with those of a dust-free $Z=0.2Z_{\odot}$, age = 50 Myr galaxy. The UV slope of dust-free models at different ages and metallicities is shown in Fig. 6.

We exploit our refined $A_{1600} - \beta$ relation, and use the average L_{UV} -SFR conversion for the objects in our sample to compute the $z \sim 3$ SFRD on the basis of available estimates of the UV luminosity function and UV slope distribution at these redshifts. We find a dust corrected $\text{SFRD} = 0.39 \text{ Msun/yr/Mpc}^3$, more than two times higher than values based on old UV slope-extinction conversions. Adopting more conservative assumptions on the age of these subsolar metallicity galaxies, we anyway find SFRD estimates 40-60% higher than those based on the standard conversion equations.

Summary & Conclusions

- The UV slope is the only dust extinction proxy available at very high redshift. UV luminosity is the best accessible SFR proxy for the most distant galaxies.
- The intrinsic UV spectrum changes with age and metallicity: proper conversions between UV slope and dust extinction, and between L_{UV} and SFR, must be based on meaningful assumptions on these two fundamental physical properties.
- To assess the reliability of the Meurer 1999 $A_{1600} - \beta$ relation, and of the Madau 1998 L_{UV} -SFR conversion, we analysed a unique sample of sources at $2.9 < z < 3.8$ for which both a spectroscopic measurement of their stellar and/or gas-phase metallicity (found to be subsolar: $0.07 < z < 0.4 Z_{\odot}$) and deep IR observations sampling their Balmer breaks (CANDELS+HUGS survey) are available.

- A comparison between SFR_{fit} (SED-fitting fixed at the measured metallicity) and the SFR_{UV99} estimated from the UV applying M99+Ma98 conversion equations shows that the latter are underestimated by a factor of 2-10 regardless of the assumed SFH.

- Other SFR indicators (radio, far-IR, X-ray, recombination lines) coherently indicate SFRs a factor of 2-4 larger than SFR_{UV99} and in closer agreement with SFR_{fit} .

- We propose a refined relation, appropriate for subsolar metallicity LBGs: $A_{1600} = 5.32 + 1.99\beta$. This relation reconciles the dust-corrected UV with the SED-fitting and the other SFR indicators.

- The fact that $z \sim 3$ galaxies have subsolar metallicity implies an upward revision by a factor of 1.5-2 of the global SFRD, depending on the assumptions about the age of the stellar populations.